Organic & Biomolecular Chemistry

Accepted Manuscript

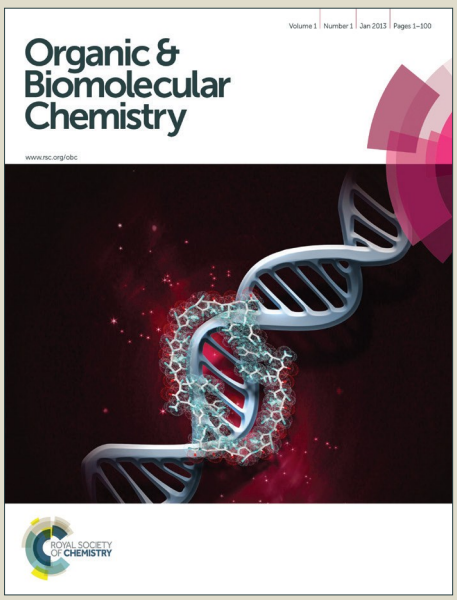

ROYAL SOCIETY OF CHEMISTRY

www.rsc.org/obc

Solvent- and Phase-Controlled Photochirogenesis. Enantiodifferentiating Photoisomerization of (*Z*)-Cyclooctene Sensitized by Cyclic Nigerosylnigerose-Based Nanosponges Crosslinked by Pyromellitate

Xueqin Wei,[a] Wenting Liang,[b] Wanhua Wu,[a] Cheng Yang,*[a] Francesco Trotta,*[c] Fabrizio Caldera,[c] Andrea Mele,[d] Tomoyuki Nishimoto[e] and Yoshihisa Inoue*[f]

Abstract

Cyclic nigerosylnigerose (CNN), a saucer-shaped cyclic tetrasaccharide with a shallow concave, was reacted with pyromellitic dianhydride in 1:2 and 1:4 ratios to give two CNN-based polymers of different degrees of crosslinking, both of which swelled upon soaking in water, behaving as 'nanosponge' (NS). These NSs evolved several phases from isotropic solution to flowing and rigid gels via suspension by gradually increasing the concentration in water. The CNN-NSs thus prepared effectively mediated the enantiodifferentiating photoisomerization of (*Z*)-cyclooctene (**1Z**) to chiral (*E*)-isomer (**1E**). The enantiomeric excess (ee) of **1E** obtained was a critical function of the solvent composition and the phase evolved at different CNN-NS concentrations in water. In isotropic solution, the enantioselectivity was generally low (-4% to +6% ee) but the chiral sense of **1E** was inverted by increasing the methanol content. Interestingly, the product's ee was controlled more dramatically by the phase evolved, as was the case with cyclodextrin-based nanosponge (CD-NS) reported previously. Thus, the ee of **1E** was low in solution and suspension, but suddenly leaped at the phase border of flowing gel and rigid gel to give the highest ee of 22-24%, which are much higher than those obtained with CD-NSs (6-12% ee), revealing the positive roles of chiral void space formed upon gelation of the crosslinked saccharide polymer.

Introduction

Catalytic photochirogenesis is one of the crucial challenging topics in current photochemistry.[1-4] Catalytic asymmetric synthesis in photochemistry has been realized mostly by chiral photosensitization, where the chirality transfer takes place in a diastereomeric exciplex intermediate formed between chiral sensitizer and prochiral substrate. Despite the considerable endeavors devoted to chiral photosensitization since the pioneering work reported by Hammond and Cole in 1965,[5] achieving high enantioselectivity in chiral photosensitization is still a nontrivial task, as can be recognized by the limited number and type of photoreactions that afford satisfactory results.[6-11] This is primarily due to the weak, short-lived and less-defined chiral environment realized in the exciplex intermediates formed in conventional chiral photosensitization systems. For a better photochirogenic performance, supramolecular photochirogenesis[2] has been proposed as a new strategy, where robust, long-lasting and well-defined chiral environment is attained not only in the ground but also in the excited state. A variety of chiral supramolecular hosts, including cyclodextrins (CDs),[12-18] chirally modified zeolite supercages,[19-21] biomolecules[22-23] and chiral hydrogen-bonding templates,[24-26] have been explored to achieve modest to excellent enantioselectivities. More recently, chiral gels[27-28] and liquid crystals[29] have also been employed as effective chiral supramolecular environment for photochirogenesis.

We have recently reported the enantiodifferentiating photoisomerizations of (Z)-cyclooctene (**1Z**) (Scheme 1) and (*Z,Z*)-1,3-cyclooctadiene (**2ZZ**) sensitized by *β*- and *γ*-CD polymers crosslinked by pyromellitate (**3-5**) (Scheme 2),[30] which were named 'nanosponges' after the swelling nature upon soaking in water and some organic solvents. These CD-based nanosponges (CD-NSs), incorporating pyromellitate linkers, not only accommodate **1Z** and **2ZZ** but also sensitize the geometrical isomerization to chiral **1E** and **2EZ** upon photoirradiation. The enantioselectivities of **1E** and **2EZ** obtained critically depended on the phase condition of CD-NS to afford the highest enantiomeric excesses (ee's) at the border of the flowing and rigid gel states. Such behavior had never been observed with non-polymeric CD-based sensitizers reported earlier.[31-35]

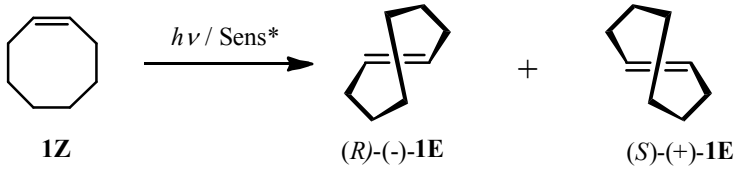

Scheme 1. Enantiodifferentiating photoisomerization of **1Z** to chiral **1E**.

A progressive aggregation mechanism has been proposed to rationalize the phase-dependent photochirogenic behavior. The inter-particle complexation of pyromellitate moiety by CD cavity exposed at the surface of CD-NS particles is considered to drive the progressive aggregations, leading to the phase transitions, upon gradual increase of the CD-NS concentration. Simultaneously, the chiral environment available for the enantiodifferentiating photosensitization is switched from the CD cavity in isotropic media to the void space surrounded by the exterior walls of CD in gel states with accompanying change in ee.[30]

To elucidate the roles of aggregation in the supramolecular photochirogenesis and also to gain further insights into the chiral sensitization mechanism in gel systems, we synthesized new pyromellitate-crosslinked saccharide polymers based on cyclic nigerosylnigerose (CNN) in this study. CNN differs from CD in number and connectivity of the building unit, being composed of only four D-glucopyranoses connected by alternating α-(1→3)- and α-(1→6)-linkages.[36-40] As a cyclic tetrasaccharide, CNN is much smaller in ring size than CDs and does not bear a confining hydrophobic cavity but a shallow concave which is not sufficient to accommodate a cyclooctene molecule. Therefore, CNN serves as an ideal saccharide building block for investigating the effects of the aggregation of NS and the void space derived therefrom upon photochirogenic behaviors, without the influence of cavity binding. Two crosslinked CNN nanosponges (CNN-NSs) **6** and **7** (Scheme 2) were prepared by crosslinking CNN with pyromellitic dianhydride (PDA) at different CNN:PDA ratios of 1:2 and 1:4, respectively.

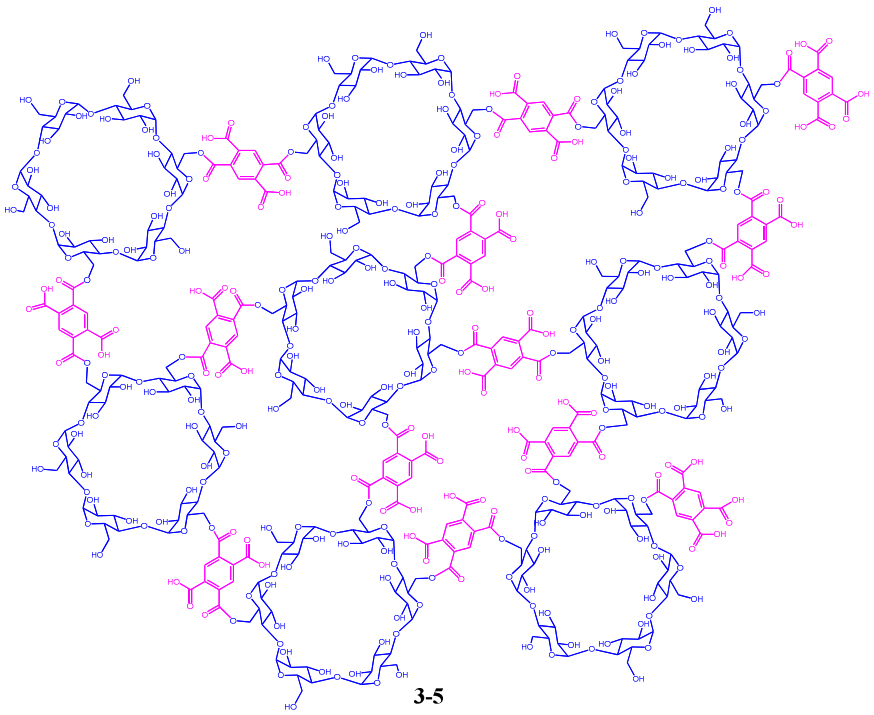

3-5

3: β-CD:PDA = 1 : 2
4: β-CD:PDA = 1 : 4
5: γ-CD:PDA = 1 : 4

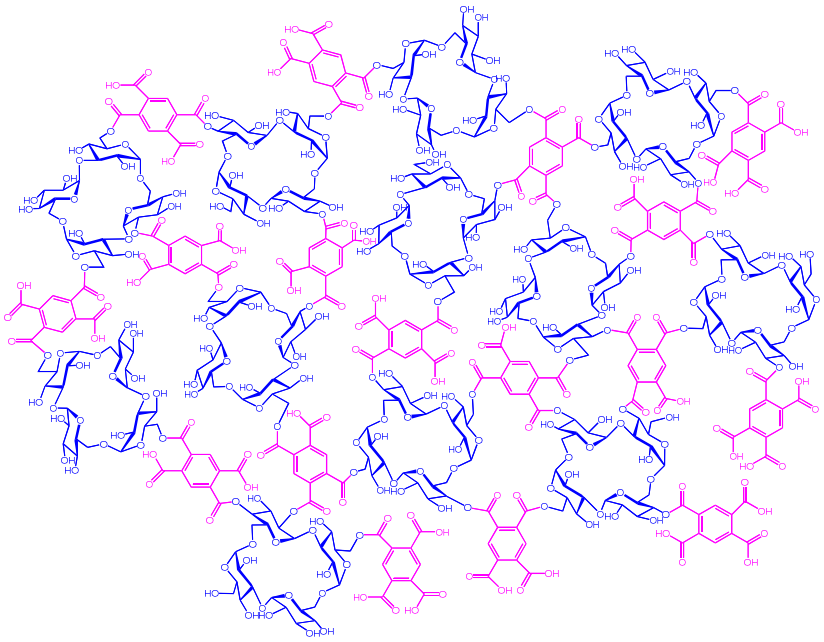

6, 7

6: CNN:PDA = 1 : 2
7: CNN:PDA = 1 : 4

Scheme 2. Chemical structures of *β*- and *γ*-CD-NSs **3-5** and CNN-NSs **6** and **7**.

Results and discussion

Photosensitization in solution

In order to evaluate the chiral environment around the pyromellitate linker, the circular dichroism spectra of CNN-NSs were measured in aqueous solutions. As can be seen from Figures 1 and 2 (red lines), both CNN-NSs **6** and **7** exhibit the induced Cotton effect signals at the main band of pyromellitate, which are however much weaker than those observed for CD-NSs **3-5** reported previously.[30] This seems reasonable as the shallow concave of CNN is not sufficient in size to fully accommodate the pyromellitate linker, allowing only weak hydrophobic interaction. Furthermore, the addition of **1Z** to an isotropic CNN-NS solution did not cause any appreciable changes in circular dichroism, probably due to the lack of confining cavity and the weak interaction in the ground state. Unlike *β*-CD that possesses a hydrophobic cavity to bind **1Z** with a relatively high affinity,[32,33] saucer-shaped CNN does not have a sufficient space for accommodating **1Z** molecule. Nevertheless, the concave is considered to be hydrophobic enough to weakly interact with **1Z** in aqueous solutions at least in the excited state. Indeed, we have shown that the optical yield of **1E** obtained in the photosensitized isomerization of **1Z** with sensitizer-appended CNN monomer in aqueous solution is appreciably higher than those obtained with α-CD-based sensitizers, indicating a positive role of the CNN concave upon photosensitization.[38] This previous result also encouraged us to investigate the photoisomerization of **1Z** sensitized by CNN-NS in aqueous solutions, despite the apparently negative result obtained upon CD spectral titration.

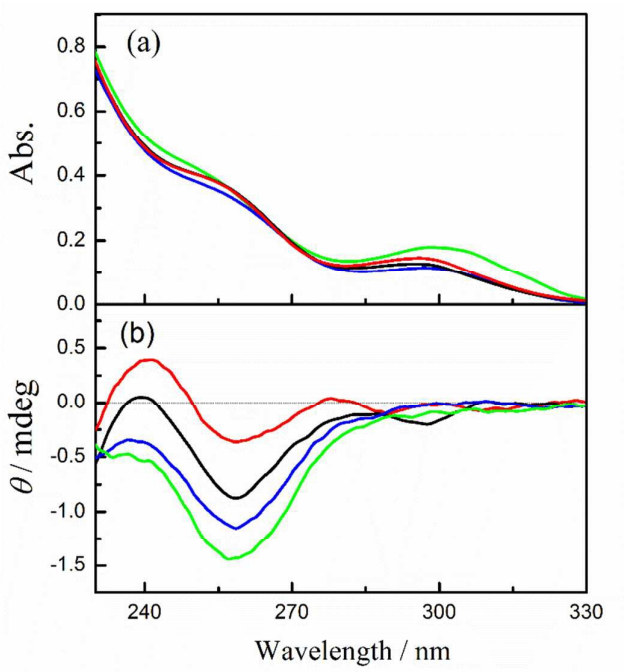

Figure 1. (a) UV-Vis and (b) circular dichroism spectra of CNN-NS **6** (0.2 mg/mL) in aqueous solutions containing 0% (red), 10% (black), 50% (blue) and 80% methanol (green).

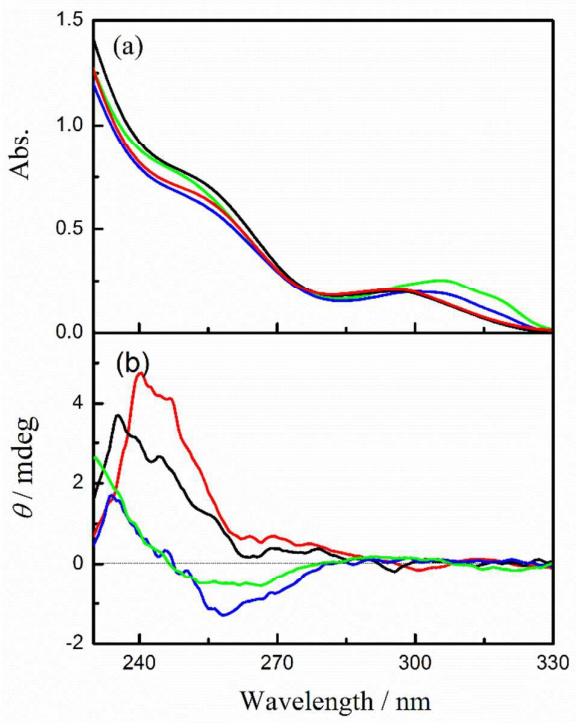

Figure 2. (a) UV-Vis and (b) circular dichroism spectra of CNN-NS **7 (**0.1 mg/mL) in aqueous solutions containing 0% (red), 10% (black), 50% (blue) and 80% methanol (green).

The enantiodifferentiating photoisomerization of **1Z** sensitized by CNN-NSs **6** and **7** was first performed in isotropic aqueous solutions containing 0-80% methanol. As shown in Table 1, the solution-phase photoisomerization of **1Z** sensitized by CNN-NS gave **1E** in modest -4% to +6% ee. Somewhat unexpectedly, the photosensitizations with **6** versus **7** afforded the opposite enantiomers of **1E** under comparable conditions. Thus, in aqueous solution at 0.5 °C, less crosslinked CNN-NS **6** afforded (*R*)-**1E** in 3.9% ee, while more cross-linked CNN-NS **7** gave antipodal (*S*)-**1E** in 4.4% ee. Intriguingly, the enantioselectivity obtained with **6** gradually deteriorated by raising the methanol content from 10% to 50% and was eventually inverted in sign (affording the antipode) to reach the highest ee of 6% in 80% methanol. It is to note that **6** and 7 share the same chiral CNN monomer unit and achiral pyromellitate linker, but differ in the degree of crosslinking and the framework rigidity. The above results reveal that the CNN-NS's chiral environment for the sensitized photoisomerization of **1Z** is readily tunable by adjusting the monomer/linker ratio or the solvent composition. Since CNN has only a shallow concave insufficient to fully include a cyclooctene molecule, the enantioselectivity achieved upon photoisomerization should rely more on the chiral environment formed by crosslinked CNN molecules, which is manipulable by the external factors such as temperature and solvent properties.

Table 1. Enantiodifferentiating photoisomerization of **1Z** sensitized by CNN-NSs **6** and **7** in aqueous solutions[a]

Host	Phase	Methanol content/%	*T*/°C	[CNN-NS] /mg mL^{-1}	Irradiation time/min	**1E**/**1Z** ratio	ee[b]/%
6	Sol	0	0.5	0.2	10	0.03	-3.9
		10	0.5	0.2	15	0.05	-2.7
			25	0.2	10	0.01	-2.5
		50	0.5	0.2	10	0.02	1.5
		80	0.5	0.2	20	0.02	5.6
					30	0.02	6.1
	Suspension	0	0.5	1	60	0.07	-2.3
				3	60	0.01	1.0
			0.5	10	60	0.15	0.1
	Flowing gel	0	0.5	30	60	0.07	4.5
				100	60	0.15	24.3
	Gel	0	0.5	150	60	0.01	6.1

7	Sol	0	0.5	0.2	10	0.07	4.4
			25	0.2	10	0.06	1.0
					30	0.13	1.0
		10	25	0.2	30	0.04	-1.0
		50	0.5	0.2	10	0.03	-3.7
					20	0.05	-3.3
			25	0.2	10	0.05	-3.6
		80	0.5	0.2	5	0.02	-1.6
	Suspension	0	0.5	1	60	0.01	0.8
				5	60	0.06	0.8
				20	60	0.06	0.4
	Flowing gel	0	0.5	100	60	0.05	5.9
				200	60	0.07	7.0
	Gel	0	0.5	350	60	0.01	21.9
				500	60	0.01	1.6

[a] Photoirradiation of **1Z** (1 mM) with **6** (0.2-150 mg/mL) or **7** (0.2-500 mg/mL) performed at 254 nm in a quartz cell under nitrogen atmosphere. [b] Enantiomeric excess of **1E** determined by chiral GC (error in ee < 0.5%); positive/negative ee values indicate preferred formation of (*S*)/(*R*)-enantiomers, respectively.

To elucidate the origin of the switching of product chirality by solvent composition, the UV-Vis and circular dichroism spectra of **6** and **7** were examined in aqueous solutions of varying methanol contents. In pure water, both **6** and **7** showed the ^1L_a and ^1L_b bands of pyromellitate at 258 nm and 295 nm, respectively; see Figures 1a an 2a. By increasing the methanol content, the ^1L_b band of **6** exhibited gradual bathochromic shifts with initial hypochromic effects up to 50% methanol, and then hyperchromic effect at 80% methanol, for which discontinuous changes in solvent structure and/or solvation mode would be responsible. Similar solvent-dependent shifts were observed also for **7** (Figure 2a). This is presumably due to the change in microenvironmental polarity experienced by the pyromellitate chromophore. Interestingly, the circular dichroism spectra of **6** and **7** were more significantly affected by the methanol content. Thus, **6** showed a small positive Cotton effect peak at 241 nm and a negative one at 259 nm in pure water. By increasing the methanol content, the whole circular dichroism signals became more negative to give a single negative extremum of -1.5 mdeg ellipticity at 258 nm in 80% methanol (Figure 1b). The UV-Vis and circular dichroism spectra of **7** showed similar trends in aqueous methanol solutions (Figure 2). These UV-Vis and

circular dichroism spectral changes indicate that increasing methanol content alters not only the microenvironmental polarity around the pyromellitate chromophore but also the conformation of the pyromellitate linker, which inevitably affects the photochirogenic behavior of CNN-NS as observed.

Thus, the solvent-induced switching of product chirality is phenomenologically well correlated with the circular dichroism spectral changes in aqueous solutions of different methanol contents. Although elucidating more detailed mechanism of the chirality inversion, including the excited-state interaction of cyclooctene substrate with pyromellitate sensitizer, would not readily be feasible, the present methodology may be employed as a convenient tool for obtaining both enantiomers upon supramolecular photochirogenesis without preparing the antipodal host, which is often unpractical when naturally occurring supramolecular hosts, such as cyclodextrin and protein, are used.

Photosensitization in gels

In our previous study on the enantiodifferentiating photoisomerization of cyclooctenes **1Z** and **2ZZ** sensitized by CD-NSs **3**-**5**,[30] we have demonstrated that the ee of **1E** and **2EZ** produced is highly sensitive to the phase of CD-NS evolved in water, which led us to a tentative conclusion that the photosensitization occurs not in the CD cavity but in the void space of NS surrounded by the exterior walls of CD. In this context, the saucer-shaped CNN, lacking an enough space for fully accommodating a cyclooctene molecule, is an ideal cyclic oligosaccharide to substitute CD for proving or disproving our hypothesis, and hence we prepared CNN-NSs **6** and **7** by crosslinking CNN with PDA under the comparable conditions employed for the synthesis of CD-NSs.[30]

The phase-transition behavior of CNN-NS was examined by gradually increasing its concentration in water at ambient temperature. As crosslinked polymers of a cyclic oligosaccharide, both **6** and **7** exhibited a stepwise phase-evolution from transparent sol to suspension, flowing gel and finally rigid gel, a behavior similar to CD-NS. Thus, CNN-NS **6** gave a homogeneous solution up to 0.4 mg/mL concentration, where transparent precipitates began to appear (Figure 3a). When the concentration was increased to 20 mg/mL, a gel-like binary phase composed of liquid and gel, or 'flowing gel' state, emerged, which was eventually converted to rigid gel at a critical gelation concentration (CGC) of 120 mg/mL.

Since the CNN concave is too shallow to strongly hold the linker moiety (i.e. pyromellitate), the host-guest complexation is not likely to play a major role in the aggregation and phase evolution of CNN-NS. As an alternative mechanism, we would propose that the inter-particle hydrogen-bonding interaction between CNN moieties and the

hydrophobic interaction of the linker moiety with the CNN's inside/outside walls are jointly responsible for the progressive aggregation of CNN-NS nanoparticles. CNN-NS **6** showed the phase transition from solution to suspension at 0.4 mg/mL concentration, which is lower than those of *β*-CD-NSs **3** and **4** but slightly higher than that of *γ*-CD-NS **5**, while the CGC of **6** is lower than those of **4** and **5**. These results suggest that the inter-particle interaction of CNN-NS does not greatly differ from that of CD-NS. Taking into account the fact that both CD-NS and CNN-NS show relatively high CGC values, we deduce that the inter-particle interaction is relatively weak for these two nanosponges, probably due to the shallow penetration of the pyromellitate moiety to CD cavity or CNN concave, as well as the relatively weak hydrogen-bonding interaction in water. Dynamic light scattering (DLS) studies confirmed a gradual growth of the particle size upon increasing the concentration of CNN-NS. As illustrated in Figure 3b, the DLS examinations revealed that **6** forms aggregates of ca. 90, 140 and >250 nm diameter at 0.2, 0.38 and 0.8 mg/mL concentrations, respectively, while visible precipitates were formed at 0.4 mg/mL concentration.

More crosslinked CNN-NS **7** showed similar stepwise phase-evolution behavior in water, but the phase transitions from solution to suspension, to flowing gel and then to rigid gel occurred at concentrations of 0.4, 50 and 350 mg/mL, respectively, each of which is higher than the corresponding value observed for less crosslinked **6**, suggesting weaker inter-particle interactions for **7**. In **7**, there should be less CNN units exposed on the surface, compared to **6**, which may discourage the inter-particle hydrogen-bonding interactions, leading to the higher phase transition concentrations. Nevertheless, CNN-NS **7** formed suspension at lower concentrations and the suspension state was kept over a wider range of concentration, compared to CD-NSs **3** and **4**.

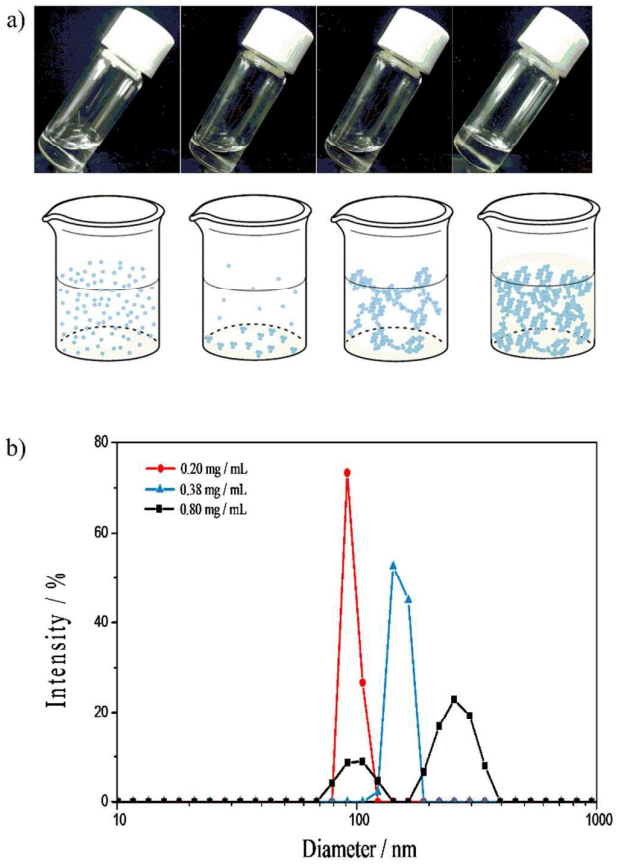

Figure 3. (a) *Upper panel*: Photographs of aqueous solutions of CNN-NS **6** at 0.2, 5, 40 and 120 mg/mL (from left to right). *Lower panel*: Schematic drawings of the phase evolution of **6**. (b) Dynamic light scattering (DLS) intensities measured at 0.20 (red), 0.38 (blue) and 0.80 (black) mg/mL concentrations of **6**.

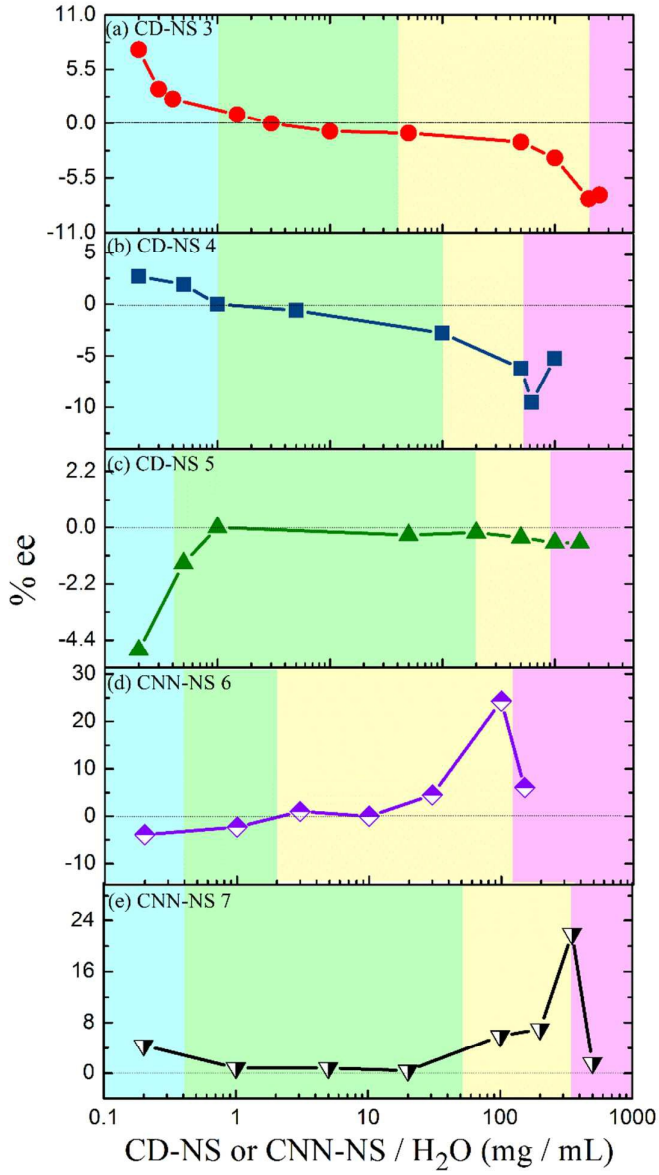

Figure 4. The ee profile of **1E** as a function of the concentration of (a) **3**, (b) **4**, (c) **5**, (d) **6** and (e) **7** upon enantiodifferentiating photoisomerization of **1Z**. The blue, green, yellow and pink regions represent the sol, suspension, flowing gel and rigid gel states, respectively.

In this relation, it is to note that the circular dichroism spectrum of **6** does not show any essential changes in shape in solution (0.2 mg/mL) and in flowing gel (120 mg/mL), excepting the small negative Cotton effect at 297 nm, as can be seen from Figure 5. This result indicates that CNN-NS nanoparticles aggregate at higher concentrations through the inter-particle interactions on the surface, while the chiral environment around the pyromellitate inside the particle is not significantly altered.

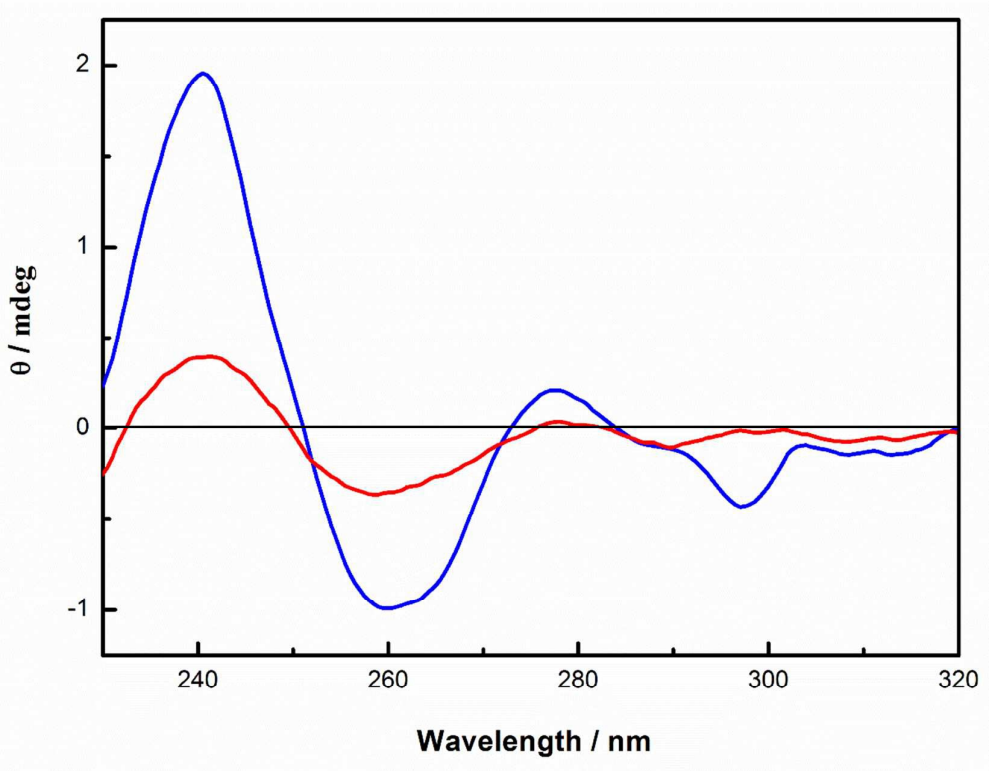

Figure 5. Circular dichroism spectra of CNN-NS **6** at 0.2 mg/mL (red line: solution in a conventional quartz cell) and at 120 mg/mL (blue line: thin layer of flowing gel sandwiched with two quartz plates).

Photoisomerization of **1Z** was sensitized by **6** and **7** in various phases prepared by changing the CNN-NS concentration. The *E/Z* ratio obtained at a relatively early stage of photoisomerization (Table 1) was significant phase-dependent, varying from 0.01 in rigid gel to 0.15 in suspension and flowing gel. The particularly low *E/Z* ratio of 0.01 in rigid gel may be attributed to the less-efficient photosensitization due to the slow diffusion of substrate to the excited sensitizer moiety within its lifetime. The enantioselectivity of **1E** produced was also a critical function of the phase of the media; see Table 1 and Figure 4. For instance, in the photoisomerization of **1Z** sensitized by **7** (Figure 4e), the ee of **1E** decreased from 4.4% to almost zero by increasing the CNN-NS concentration from 0.2 to 1 mg/mL, with accompanying phase transition from sol to suspension, and stayed low throughout the suspension region (0.4-50 mg/mL), but jumped up to 21.9% at the border of the flowing and rigid gel regions. A similar phase-dependent ee profile was observed upon sensitization with **6** (Figure 4d), affording an even higher ee value of 24.3% near the border of the flowing and rigid gel regions. These ee profiles are consistent in general with those obtained with CD-NSs

3 and **4**[30] (Figures 4a and 4b), but significantly differ from the ee profile obtained with γ-CD-NS **5** (Figure 4c), which possesses a much larger CD cavity than **3** and **4** and gives nearly racemic product in all the anisotropic phases.[30] These resembling photochirogenic behaviors suggest operation of conceptually the same enantiodifferentiation mechanism in both CNN-NS and CD-NS photosensitizations.

It is noteworthy that CNN-NSs, possessing no confining cavity but a shallow concave, afford **1E** in such good ee's as 22-24% in gel states, which far exceed the ee values of 6-14% obtained with CD-NSs[30] under comparable conditions. This result reinforces our previous claim that not the individual host cavity but the polymer void surrounded by the host's exterior walls is responsible for the chiral induction in the supramolecular photosensitization in crosslinked CD and CNN gels.[30] In the present case, the concaved shape of CNN may provide a better chiral environment for effective enantiodifferentiating photoisomerization of **1Z** sensitized by pyromellitate crosslinker located nearby. It is interesting that CNN's concave itself is not sufficient to tightly hold the substrate molecule and indeed only poor ee was obtained upon enantiodifferentiating photosensitization in isotropic solution,[32] whereas CNN aggregates formed in polymer gel show much better photochirogenic performance. Thus, the originally poor chirality-transfer ability of CNN-NS was significantly improved by supramolecular aggregation, for which the closer contacts with the CNN' inside and/or outside walls as well as the well-ordered, but less-dynamic nature of the gel are likely to be jointly responsible.

Conclusion

In this work, we have employed cyclic tetrasaccharide CNN as a 'pseudo' or 'hemi' host that lacks a confining cavity to fully accommodate a guest substrate. Our immediate task was to assess and compare the photochirogenic performances of the CNN's shallow concave at the molecular level in isotropic solution and also at the supramolecular level in aggregates. A more crucial task was to critically examine our previous claim that the chiral polymer void formed upon aggregation of cyclic oligosaccharide hosts plays the major roles in determining the stereochemical outcomes of supramolecular photochirogenic reactions.

For these purposes, we synthesized two CNN-based nanosponges of different degrees of crosslinking (**6** and **7**) and employed them as chiral supramolecular sensitizers for mediating the enantiodifferentiating photoisomerization of **1Z** to **1E** in aqueous solutions containing 0-80% methanol. The enantioselectivity of **1E** obtained was highly sensitive to the solvent composition and the degree of crosslinking, exhibiting a switching of the product chirality,

which provides us with a convenient tool for manipulating the photochirogenic outcomes. Both **6** and **7** showed the phase evolution from sol to rigid gel by increasing the CNN-NS concentration in water. Interestingly, the product's ee was a critical function of the phase of CNN-NS to achieve the highest enantioselectivity at the phase border of flowing and rigid gels. This result unambiguously reveals that the polymer void surrounded by the exterior walls of host is the source of chirality transfer upon photosensitization with CD- and CNN-NSs. The concept and methodology developed in this study are not restricted to the present system, but expandable to other substrates and photochirogenic reactions by choosing suitable sensitizing crosslinker and chiral building block.

Experimental Section

Instruments

UV- Vis and circular dichroism spectra were obtained on JASCO V-650, and JASCO J-A500-150 spectrometers, respectively. DLS measurements were performed on a Zetasizer Nano S90 (Malvern Instruments, Worcestershire, UK) instrument.

Materials

CNN was obtained from Hayashibara Co., Inc. Cyclooctene was purchased from Tokyo Chemical Industries and used after fractional distillation. Other chemicals were commercially available and used without further purification.

CNN-NSs **6** and **7** were synthesized and purified according to essentially the same procedures employed for the preparation of CD-NSs **3**-**5**.[30] Thus, 2.0 g of CNN (dried at 100°C in an oven, until a constant weight was reached) were dissolved in 8 mL of DMSO with continuous stirring, to which were added 2 mL of triethylamine and, 5 min later, 1.345 g (for **6**) or 2.691 g (for **7**) of pyromellitic dianhydride. The mixture was allowed to react at room temperature, while the gelation began in a few seconds after the addition of crosslinker. After 24 h, the crosslinking appeared to complete, affording a monolithic block, which was ground in a mortar, washed with deionized water and rinsed with acetone in a Buchner funnel with an aspirator. The polymer residue was air-dried and extracted with acetone for 14 h in a Soxhlet apparatus to give CNN-NS **6** (4,3 g, 97% yield) or **7** (5,8 g, 96% yield) as white powder. These samples, which were practically insoluble (but swelled) in water and many organic solvents, gave the satisfactory elemental analyses, ATR-FTIR spectra, and thermogravimetric analyses shown in ESI.

Photolysis

Sample solution containing **1Z** and CNN-NS in a quartz cell was placed in a UNISOKU CoolSpek USP-203CD cryostat, purged with nitrogen gas, and irradiated at a given temperature at 254 nm with a 20-W low pressure mercury lamp (UVL20PH-6). No appreciable phase change or transition was observed after irradiation. The photolyzed sample was added to 10% aqueous KOH solution (2 mL), and the resulting mixture was extracted with pentane (1 mL). An aliquot of the pentane extract was analyzed by gas chromatography (GC) on a Shimadzu CBP-20 (PEG) column for E/Z ratio. To determine the ee value, an aqueous silver nitrate solution (2 mL) was added to the organic extract at 0 °C to give a stable Ag^+ complex with **1E**. The aqueous solution of [Ag^+ **1E**] complex was washed twice with pentane (1 mL) and added to a 28% aqueous ammonia solution at 0 °C to liberate **1E**. Finally, the liberated cyclooctene was extracted with pentane (0.3 mL), and the pentane extract was analyzed by GC on a Supelco β-DEX 225 column.

Acknowledgements

This work was supported by National Natural Science Foundation of China (No. 21372165 and 21321061), State Key Laboratory of Polymer Materials Engineering, Grant No. sklpme2014-2-06, Comprehensive Training Platform of Specialized Laboratory, College of Chemistry, Sichuan University and Japan Society for the Promotion of Science (No. 21245011 and 26620030).

Notes and References

[a] *College of Chemistry, State Key Laboratory of Biotherapy, West China Medical School and State Key Laboratory of Polymer Materials Engineering, Sichuan University, 29 Wangjiang Road, Chengdu 610064, China. E-mail: yangchengyc@scu.edu.cn*

[b] *Institute of Environmental Sciences, Shanxi University, Taiyuan 030006, China*

[c] *Department of Chemistry, University of Torino, Via P. Giuria 7, 10125 Torino, Italy. E-mail: francesco.trotta@unito.it*

[d] *Department of Chemistry, Materials and Chemical Engineering "Giulio Natta", Politecnico di Milano, Piazza L. Da Vinci 32, 20133 Milano, Italy*

[e] *Hayashibara Co., 675-1 Fujisaki, Naka-ku, Okayama 702-8006, Japan*

[f] Department *of Applied Chemistry, Osaka University, 2-1Yamada-oka, Suita 565-0871, Japan. E-mail: inoue@chem.eng.osaka-u.ac.jp*

† Electronic Supplementary Information (ESI) available: Elemental analysis, ATR-FTIR spectral and thermogravimetric analysis data for CNN-NSs **6** and **7**.

1. Y. Inoue and V. Ramamurthy, *Chiral Photochemistry*, Dekker, New York, 2004.
2. C. Yang and Y. Inoue, *Chem. Soc. Rev.*, 2014, **43**, 4123.
3. A. G. Griesbeck and U. J. Meierhenrich, *Angew. Chem. Int. Ed.,* 2002, **41**, 3147.
4. C. Müller and T. Bach, *Aust. J. Chem.* 2008, **61**, 557.
5. G. S. Hammond and R. S. Cole, *J. Am. Chem. Soc.*, 1965, **87**, 3256.
6. Y. Inoue, T. Yokoyama, N. Yamasaki and A. Tai, *Nature*, 1989, **341**, 225.
7. Y. Inoue, H. Ikeda, M. Kaneda, T. Sumimura, S. R. L. Everitt and T. Wada, *J. Am. Chem. Soc.*, 2000, **122**, 406.
8. A. Bauer, F. Westkaemper, S. Grimme and T. Bach, *Nature*, 2005, **436**, 1139.
9. R. Brimioulle and T. Bach, *Science* 2013, **342**, 840。
10. J. Sivaguru, A. Natarajan, L. S. Kaanumalle, J. Shailaja, S. Uppili, A. Joy and V. Ramamurthy, *Acc. Chem. Res.*, 2003, **36**, 509.
11. H. Saito, T. Mori,T. Wada and Y. Inoue, *J. Am. Chem. Soc.*, 2004, **126**, 1900.
12. C. Yang, *Chin. Chem. Lett.*, 2013, **24**, 437.
13. Y. Inoue, S. F. Dong, K. Yamamoto, L.-H. Tong, H. Tsuneishi, T. Hakushi and A. Tai, *J. Am. Chem. Soc.*, 1995, **113**, 2793.
13. C. Yang, T. Mori, Y. Origane, Y. H. Ko, N. Selvapalam, K. Kim and Y. Inoue, *J. Am. Chem. Soc.*, 2008, **130**, 8574.
14. C. Yang, C. Ke, W. Liang, G. Fukuhara, T. Mori and Y. Liu,; Inoue, Y. *J. Am. Chem. Soc.* 2011, **133**, 13786.
15. J. Yao, Z. Yan, W. Wu, C. Yang, M. Nishijima, G. Fukuhara, T. Mori and Y. Inoue, *J. Am. Chem. Soc.*, **2014**, 136，6916.
16. Q. Wang, C. Yang, C. Ke, G. Fukuhara, T. Mori, Y. Liu and Y. Inoue, *Chem Commun*, 2011, **47**, 6849.
17. G.-H. Liao, L. Luo, H.-X. Xu, X.-L. Wu, L. Lei, C.-H. Tung and L.-Z. Wu, *J. Org. Chem.*, 2008, **73**, 7345.
18. L. Luo, S.-F. Cheng, B. Chen, C.-H. Tung and L.-Z. Wu, *Langmuir*, 2010, **26**, 782.
19. A. Joy, S. Uppili, M. R. Netherton, J. R. Scheffer and V. Ramamurthy, *J. Am. Chem. Soc.*, 2000, **122**, 728.
20. J. Sivaguru, T. Shichi and V. Ramamurthy, *Org. Lett.*, 2002, **4**, 4221.
21. J. Sivaguru, S. Jockusch, N. J. Turro and V. Ramamurthy, *Photochem. Photobiol. Sci.*, 2003, **2**, 1101.
22. S. Asaoka, T. Wada and Y. Inoue, *J. Am. Chem. Soc.*, 2003, **125**, 3008.
23. M. Nishijima, T. Wada, T. Mori, T. C. S. Pace, C. Bohne and Y. Inoue, *J. Am. Chem. Soc.*, 2007, **129**, 3478.
24. J. Mizoguchi, Y. Kawanami, T. Wada, K. Kodama, K. Anzai, T. Yanagi and Y. Inoue, *Org. Lett.*, 2006, **8**, 6051.
25. T. Bach, H. Bergmann, B. Grosch and K. Harms, *J. Am. Chem. Soc.*, 2002, **124**, 7982.
26. C. Müller, A. Bauer, M. M. Maturi, M. C. Cuquerella, M. A. Miranda and T. Bach, *J. Am. Chem. Soc.*, 2011, **133**, 16689.
27. A. Dawn, T. Shiraki, S. Haraguchi, H. Sato, K. Sada and S. Shinkai, *Chem. Eur. J.*, 2010, **16**, 3676.
28. M. Shirakawa, N. Fujita, T. Tani, K. Kaneko and S. Shinkai, *Chem. Commun.*, 2005, 4149.
29. Y. Ishida, Y. Kai, S.-y. Kato, A. Misawa, S. Amano, Y. Matsuoka and K. Saigo, *Angew.*

Chem. Int. Ed., 2008, **47**, 8241.
30. W. Liang, C. Yang, D. Zhou, H. Haneoka, M. Nishijima, G. Fukuhara, T. Mori, F. Castiglione, A. Mele, F. Caldera, F. Trotta and Y. Inoue, *Chem. Commun.*, 2013, **49**, 3510.
31. C. Yang, T. Mori, T. Wada and Y. Inoue, *New J. Chem.*, 2007, **31**, 697.
32. W. Liang, C. Yang, M. Nishijima, G. Fukuhara, T. Mori, A. Mele, F. Castiglione, F. Caldera, F. Trotta and Y. Inoue, *Beilstein J. Org. Chem.*, 2012, **8**, 1305.
33. R. Lu, C. Yang, Y. Cao, Z. Wang, T. Wada, W. Jiao, T. Mori and Y. Inoue, *J. Org. Chem.*, 2008, 7695.
34. R. Lu, C. Yang, Y. Cao, Z. Wang, T. Wada, W. Jiao, T. Mori and Y. Inoue, *Chem. Commun.*, 2008, 374.
35. G. Fukuhara, T. Mori, T. Wada and Y. Inoue, *Chem. Commun.*, 2005, 4199.
36. P. Biely, G. L. Cote and A. Burgess-Cassler, *Eur. J. Biochem.* 1994, **226**, 633.
37. G. L. Cote and P. Biely, *Eur. J. Biochem.* 1994, **226**, 641.
38. T. Nishimoto, H. Aga, K. Mukai, T. Hashimoto, H. Watanabe, M. Kubota, S. Fukuda, M. Kurimoto and Y. Tsujisaka, *Biosci. Biotech. Biochem.*, 2002, **66**, 1806.
39. H. Aga, T. Nishimoto, M. Kuniyoshi, K. Maruta, H. Yamashita, T. Higashiyama, T. Nakada, M. Kubota, S. Fukuda, M. Kurimoto and Y. Tsujisaka;, *J. Biosci. Bioeng*., 2003, **95**, 215.
40. C. Yang, W. Liang, M. Nishijima, G. Fukuhara, T. Mori H. Hiramatsu, Y. Dan-oh, K. Tsujimoto and Y. Inoue, *Chirality*, 2012, **24**, 921.

TOC Graphic